VERSITA

Cent. Eur. J. Chem. • 11(8) • 2013 • 1264-1277
DOI: 10.2478/s11532-013-0259-7

Central European Journal of **Chemistry**

L-leucinium perchlorate: new molecular complex with nonlinear optical properties. Vibrational, calorimetric and theoretical studies

Research Article

Mariusz K. Marchewka*, Marek Drozd

Institute of Low Temperature and Structure Research Polish Academy of Sciences, 50-422 Wrocław, Poland

Received 30 September 2012; Accepted 14 March 2013

Abstract: On the basis of prior X-ray crystallographic results published by J. Janczak and G. Perpetuo, detailed vibrational studies were performed. The FT-IR and Raman spectra at ambient temperature were measured. The NLO properties were determined with the Kurtz-Perry experiment.

Theoretical vibrational spectra were calculated. A detailed potential energy distribution (PED) analysis was performed. Assignments of observed bands were made. On the basis of these results, the behaviour of hydrogen bonds in the investigated compound was analysed and discussed. The equilibrium geometry of L-leucinium perchlorate was obtained. The results were compared with experimental X-ray data. The DFT formalism was used in theoretical studies.

Detailed TDDFT study of hyperpolarizbility of first and second order for the investigated molecule was performed. Results were compared with experiments. Theoretical population analysis was used to determine the local electron density and local charges in investigated molecule. Differential scanning calorimetric study (DSC) was performed.

Keywords: *L-leucinium perchlorate • Vibrational spectra • Hydrogen bonding • Density Functional Theory • Nonlinear Optics*

1. Introduction

During past two decades, attention has been focused on the design and application of new chromophores that may be included into inorganic hosts [1,2]. The salts of protonated amino acids are representative for such compounds, and the interest of these compounds has been increased recently after the discovery of perspective NLO properties in a crystal of L-arginine phosphate monohydrate (LAP) [3-7]. The possible class of organic salts of aminoacids is the class of iodates [8]. These recently synthesized iodates of arginine and lysine, bis(hydrogeniodate) of arginine and tris(hydrogeniodate) of lysine exhibit nonlinear optical properties [9].

In order to have nonlinear optical properties the compounds should possess some general structural, vibrational and electronic characteristics. For specific compounds (push-pull polyenes) it is possible to confirm by analysis of their vibrational spectra the key role played by the structural parameters of the polyene chain in determining the nonlinear optical response. The observation of the mutual exclusion rule that is obeyed for non-centrosymmetric structure is also evidence for SHG activity of studied crystals. The lack of macroscopic centre of inversion is the *conditio sine qua non* for the crystal to be SHG active. It is desirable to have a small HOMO-LUMO gap for a material exhibiting second order nonlinear phenomena.

Some simple organic and inorganic salts of aminoacids appear to be promising materials for optical second harmonic generation (SHG). Moreover, such crystals display other interesting physical and chemical properties, namely ferroelectric, antiferroelectric and ferroelastic phase transitions as well as phases with commensurate and incommensurate superstructures [10,11].

* *E-mail: dariusz482@kn.pl*

Recently, the complexes of L-leucine with inorganic and organic acids were investigated. The detailed studies are currently focused on the role of hydrogen bond system in phase transitions and NLO behaviour.

Detailed FTIR and FT Raman studies for L-leucine-selenic acid (ratio 1:2) were performed [12]. The infrared and Raman spectra for both protiated and deuteriated compounds were measured and interpreted. The infrared spectra were studied down to temperatures of 90 K. According to these results, Nemec *et al.* [12] suggest that the crystal structure of this compound is determined by extensive hydrogen bonding network. The investigated crystal is stable in the temperature range 95-445 K. No phase transitions were found during the DSC measurement.

L-leucinium oxalate was studied by Rajagopal *et al.* [13]. In the investigated compound, the leucine molecule exists in cationic form, with a protonated amino group and an uncharged carboxylic group. Pseudo-inversion centres relate the leucinium cations and semi-oxalate anions. The leucinium and semi-oxalate ions form hydrogen bonded double layer chains. Additionally, the leucinium cations are arranged in these double layers on opposite sides leading to alternating hydrophobic and hydrophilic layers. The extended investigation of this compound performed by Anbuchezhiyan *et al.* [14] confirms that this monocrystal belongs to the noncetrosymmetric space group and reveals the NLO properties.

The structure of L-leucinium picrate was published by Anitha *et al.* [15]. The asymmetric unit of the investigated compound contains two nonprotonated leucine residues, two protonated leucinium cations and two picrate anions. The leucine residues show a class II hydrogen bonding scheme, and the leucinium residues show a class I hydrogen bonding scheme. The leucine and leucinium residues form infinite hydrogen bonded chains. The crystal belongs to noncetrosymmetric crystallographic space group and is potential NLO material.

The crystal structure of L-leucinium perchlorate was determined by Janczak *et al.* [16]. The asymmetric unit consists protonated L-leucinium cations and perchlorate anions. L-leucinium cations related by a twofold screw axis are interconnected by N-(HO)-O hydrogen bonds into zigzag chains parallel to [010]. The O atoms of the perchlorate anions act as acceptors of hydrogen bonds that link L-leucinium chains into separated but interacting two-dimensional layers. As this is non-centrosymmetric crystal, the *conditio sine qua non* for second harmonic generation is fulfilled in this case.

We report the results of the detailed vibrational experimental and theoretical studies for L-leucinium perchlorate. The powder IR and Raman spectra at ambient temperature were measured. The relationship between structure and vibrational spectra was analysed with special attention paid on the hydrogen bonding system.

The full PED analysis and assignment of most characteristic bands is performed with simultaneous comparison with experimental spectra. This part of work could be helpful in design of new complexes with expectations specified in details.

Furthermore, the time dependent Hartee-Fock calculations [28] of NLO properties and dipole moments were performed and relation to experimental values of b is discussed.

2. Experimental procedure

2.1. Vibrational measurements

The FTIR powder spectra were measured as Nujol suspensions using a Bruker IFS-88 spectrometer with a resolution 2 cm^{-1}. For elimination of the side lobes that result after truncating the interferogram with a boxcar function, the Norton-Beer weak apodization function was used. The samples were put between KBr windows.

The Raman spectra at room temperature were measured with the FRA-106 Raman module attached to Bruker IFS-88 (Nd:YAG laser, 1064 nm, 150 mW, resolution 2 cm^{-1}).

2.2. DSC measurements

Differential scanning calorimetric measurements were performed on Perkin-Elmer DSC-7 calorimeter equipped with the CCA-7 low temperature attachment with a heating/cooling rate 20° min^{-1}. The samples of the mass *ca.* 20 mg were sealed in the aluminum pans. The measurements were performed for the temperature region 100 – 350 K.

2.3. Kurtz Perry powder test

SHG experiment was carried out using Kurtz-Perry powder technique described in [23]. The calibrated samples (studied and KDP) were irradiated at 1064 nm by Nd+:YAG laser (Quanta Ray DCR-11) and the second harmonic beam power diffused by the powder sample (at 532 nm) was measured as a function of the fundamental beam power.

2.4. Theoretical

The optimized equilibrium structure for L-leucinium perchlorate has been calculated by DFT method [28,34] with 6-311++G(d,p) basis set [31]. The harmonic frequencies and infrared intensities were calculated using B3LYP method with 6-311++G(d,p) basis set.

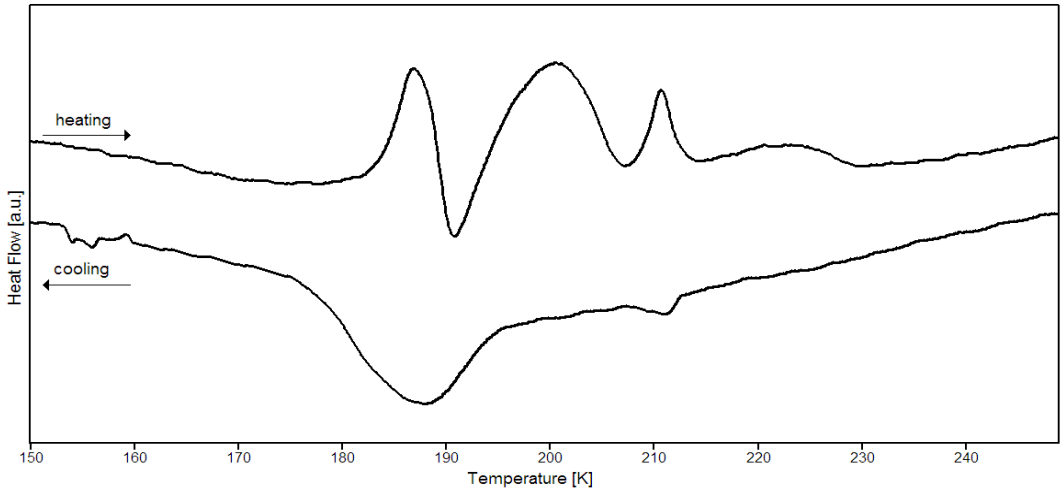

Onset heating	Onset cooling	Enthalpy [J mol^{-1} K^{-1}] (at heating)
191	194	0.62
209	213	0.00892
183		0.31

Figure 1. The DSC diagram for L-leucine*perchlorate acid complex.

The normal coordinate analyses have been carried out for L-leucinium perchlorate according to the procedure described and recommended by Fogarasi and Pulay [17]. Scaling factor for frequencies of stretching vibrations (0.983) was determined on the basis of previously studied similar organic systems [18,35]. The calculated potential energy distribution for L-leucinium perchlorate has enabled us to make detailed band assignment in infrared spectra.

The nonlinear optical response of an isolated molecule in an electric field $E_i(w)$ can be presented as a Taylor series expansion of the total dipole moment, m_t, induced by the field $\mu_t = \mu_0 + \alpha_{ij}E_i + \beta_{ijk}E_iE_j + ...$ where a is a linear polarizibility, m_0 is permanent dipole moment, and b_{ijk} are the first hyperpolarizability tensor components. The NLO response of the material in molecular state can be determined by computation and by measuring it experimentally. The values obtained by different methods may be different; therefore it is necessary to give an exact definition [1]. In this paper we will use the calculation method of dynamical hyperpolarizability implemented in GAMESS [30-31] program.

Calculations of the first hyperpolarizability by quantum chemical methods were carried out using RHF method with 6-311++G(d,p) basis set.

All calculation was performed with the GAMESS program, version from 12 December 2003 (R2) compiled under Linux operating system.

3. Results and discussion

3.1. DSC studies

The calorimetric investigations were carried out in the aim the define of thermal durability of the sample. The thermal stability (especially in high temperature) is very important in real NLO applications. The DSC diagram for titled compound with the all experimental parameters is presented in Fig. 1. The first DSC measurement shows during the cooling cycle the two discontinuities. The first one appears at 194 K. On the DSC curve, the characteristic peak is observed. It shows that a non-continuous or second order phase transition occurs. The enthalpy calculated for this peak is equal to *ca.* 0.50 J mol^{-1} K^{-1}. The second peak is observed at 213 K, but the enthalpy in this case is very small. Heating cycle shows tree big peaks at 191, 209 and 183 K, respectively. The calculated enthalpy for peak at 191 K is equal to 0.62 J mol^{-1} K^{-1}, whereas for second anomaly the enthalpy is smaller (0.31 J mol^{-1} K^{-1}. The smallest value of enthalpy is observed for peak at 209 K (0.0089 J mol^{-1} K^{-1}).

It should be emphasized that the discontinuities observed during the heating and cooling cycles are not compatible and cannot be described as typical phase transitions phenomena. The next cycles of experiment were carried out on fresh sample. The heating and cooling experiment indicates discontinuities with various

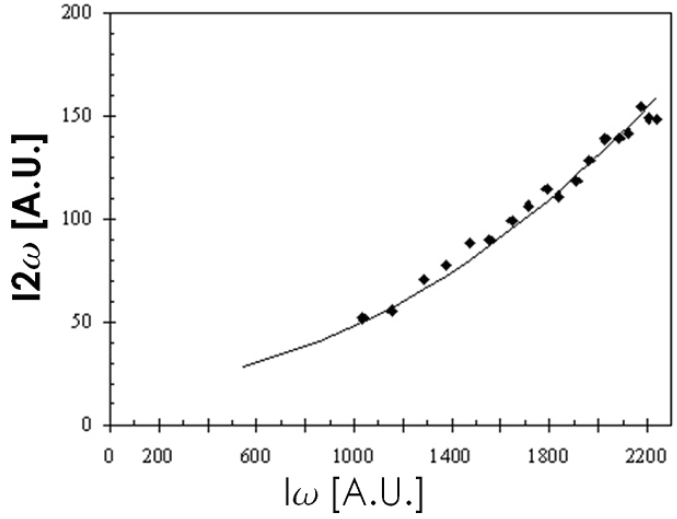

Figure 2. The Kurtz-Perry experimental data for L-leucinium perchlorate.

characters. The differences in temperature of observed anomalies between first and second experiment were noticed. The values of enthalpy are substantially different, too. According to DSC measurements it is not clear that the phase transitions are observed or not.

It ought to be mentioning here that for most perchlorates DSC experiment shows the discontinuities on the curves in the temperature range 150 – 250 K. Its origin may be connected with disordered perchlorate anions present in the crystal structure [36].

3.2. NLO studies

The first hyperpolarizability b values obtained from theoretical calculation are collected in the Table 1. All results are given in the molecular internal coordinate system represented by (x, y, z) whereby the indices x, y and z refer to the three axes corresponding to the components of moment of inertia in increasing order.

For L-leucinium perchlorate the value of vector part of b, calculated at fundamental wavelength of 1064 nm, is equal to 62.31 (10^{-30} esu). The hyperpolarizability b_{vec} is dominated by b_x component having 59.98 (10^{-30} esu). Domination of particular component indicates a substantial delocalization of charge in this direction (X). The values of b in other directions are in the range of 0.44 (b_{ZYZ}) – 15.44 (b_{XXX}) (10^{-30} esu). These values of hyperpolarizabilty are relatively big, comparable with 4-nitroaniline standard (38.8×10^{-30} esu). The values are comparable with data obtained for some melaminium compound [37]. On the basis of previous calculation the results of theoretical b hyperpolarizability seems to *ca.* two times larger as in KDP standard.

The SHG experiment was carried out using the Kurtz-Perry method at 1064 nm by Nd:YAG laser. The results are shown in the Fig. 2. The measured points (second harmonic beam power diffused by the samples at 532 nm was measured as a function of the fundamental beam power) of this experiment lie on the parabolic curve. It is necessary for materials with true second harmonic generation. The experiment shows that the experimental SHG efficiency of studied compound is comparable with theoretical calculations.

Comparison of theoretical and experimental results strongly suggests that SHG effect in this crystal is not significantly influenced by intermolecular hydrogen bonds interactions, because the calculations of l b hyperpolarizability were performed for one formal molecule.

According to the above observations, L-leucinium perchlorate seems to be promising material for nonlinear optical applications. Strong delocalization of vibrational energy on internal coordinates (*cf.* values of PED in Table 4) allows the system to change polarisability easily, hence to show pronounced nonlinear optical effect, as is observed.

3.3. Natural population analysis

Natural (localized) orbitals are used in computational chemistry to calculate the distribution of electron density in atoms and in bonds between atoms. This information is critical for estimate of strength of bonds in molecule. On the other hand the distribution of charges in investigated system can be used for design of new molecules with similar properties. On the basis of these results the nucleophilic or electrophilic character of investigated molecule is determined. The results of NBO analysis [34] are presented in the Table 2. Almost all carbon atoms of L-leucine molecule have negative

Table 1. Calculated SHG generation.

Table 5: b (SECOND HARMONIC GENERATION): b(-2w;w,w)		
b	Static [10^{-30} esu]	SHG at 1064nm [10^{-30} esu]
XXX	14.66	15.44
YXX	1.85	1.88
ZXX	1.97	2.08
XXY	1.85	1.91
YXY	2.77	3.01
ZXY	1.03	1.04
XXZ	1.97	2.06
YXZ	1.03	1.02
ZXZ	1.41	1.54
XYY	2.77	2.99
YYY	-3.18	-3.43
ZYY	-1.54	-1.69
XYZ	1.03	1.06
YYZ	-1.54	-1.72
ZYZ	0.49	0.46
XZZ	1.41	1.56
YZZ	0.49	0.47
ZZZ	4.81	5.17
X	56.54	59.98
Y	-2.52	-3.20
Z	15.70	16.58
V	58.73	62.31
MOMENTS OF INERTIA [AMU-Å^2): IXX = 376.288; IYY = 1981.145; IZZ = 2000.350		

charges (C1, C2, C3, C4, C5). These charges are in the range -0.7 - -0.17 e. Negative charge is observed for nitrogen (N6) of NH_3 group, also. In the case of C7 atom the positive charge. For all hydrogen atoms the calculated charges are positive. The biggest vale is noticed for hydrogen atom H15 (*ca.* 0.53 e), which is connected with oxygen atom of COO group. It should be noticed that for all functional groups in L-leucine molecule the charge distribution is very symmetrical. In both methyl groups (CH_3) the charges of all hydrogen atoms are equal. Small differences are noticed in the case of amino group (NH_3). The calculated values of charges for hydrogen atoms are in the range (0.49 – 0.47 e). Similar situation is observed for ethyl group (CH_2). The NBO values are equal to *ca.* 0.25 – 0.27 e.

The NBO studies for oxygen atom of COOH are typical for this type of functional group. For the oxygen atom connected with hydrogen the is significantly smaller than noticed for (O9) oxygen atom linked with carbon by double chemical bond.

The charge calculated for Cl atom of perchlorate anion is positive. The values of charges for oxygen atom (O10 and O13) are practically equal, (both negative). Two other oxygen atoms (O12 and O14) have negative charges a little bit different. It should be noticed that sum of negative charge for oxygen atom is equal to *ca.* -3.3 e, whereas the positive charge of Cl atom is equal to 2.44 e, only. This discrepancy suggests that in the case of O10 and O13 oxygen atoms, the additional nucleophilic substitution can be observed.

3.4. Equilibrium geometry

Comparison of theoretical calculation with experimental X-ray data for bond lengths of L-leucine skeleton shows very good agreement. The equilibrium geometry together with experimental X-ray structure of investigated molecule is presented on Fig. 3. The conformation of the title compound in the gas phase is close to the real structure.

All C-C distances are identical in both cases (see Table 3). A small difference is observed in the case of C5-N6 bond. The experimental value is equal to 1.53 Å, whereas in theoretical calculation this length is a little bit shorter and equal to 1.50 Å. Similar results were obtained for C-O bonds of COOH group. The C7-O9 bond has identical length in theoretical and experimental data. Small discrepancy is observed for C7-O8 bond. In this case the theoretical value is longer than observed in X-ray experiment (1. 34 Å and 1.32 Å), but this difference is within the range of experimental error.

All C-H distances obtained from X-ray experiment are practically identical. These values are in the range 0.96 – 0.98 Å. It strongly suggests that in X-ray experiment the position of hydrogens were obtained [15] from assumption geometry. In this case the error in considered C-H bond lengths may be present. The values obtained from theoretical calculations can be more adequate. For all C-H bonds the theoretical values are bigger. These bond lengths are in the range 1.09 – 1.10 Å. Similar relationship is observed in the case of N-H bonds. According to theoretical data these bond lengths are not identical. The shortest values are noticed for N6-H19 and N6-H17 bonds (1.02 Å and 1.03 Å, respectively). Third bond (N6-H18) is significantly longer and equal to 1.07 Å.

It should be emphasized that the biggest discrepancy between theoretical and experimental values are noticed for perchlorate anion. Generally, the theoretical values are significantly bigger than experimental one. The perchlorate anion shows distortion from the tetrahedral geometry in both experimental and theoretical approach

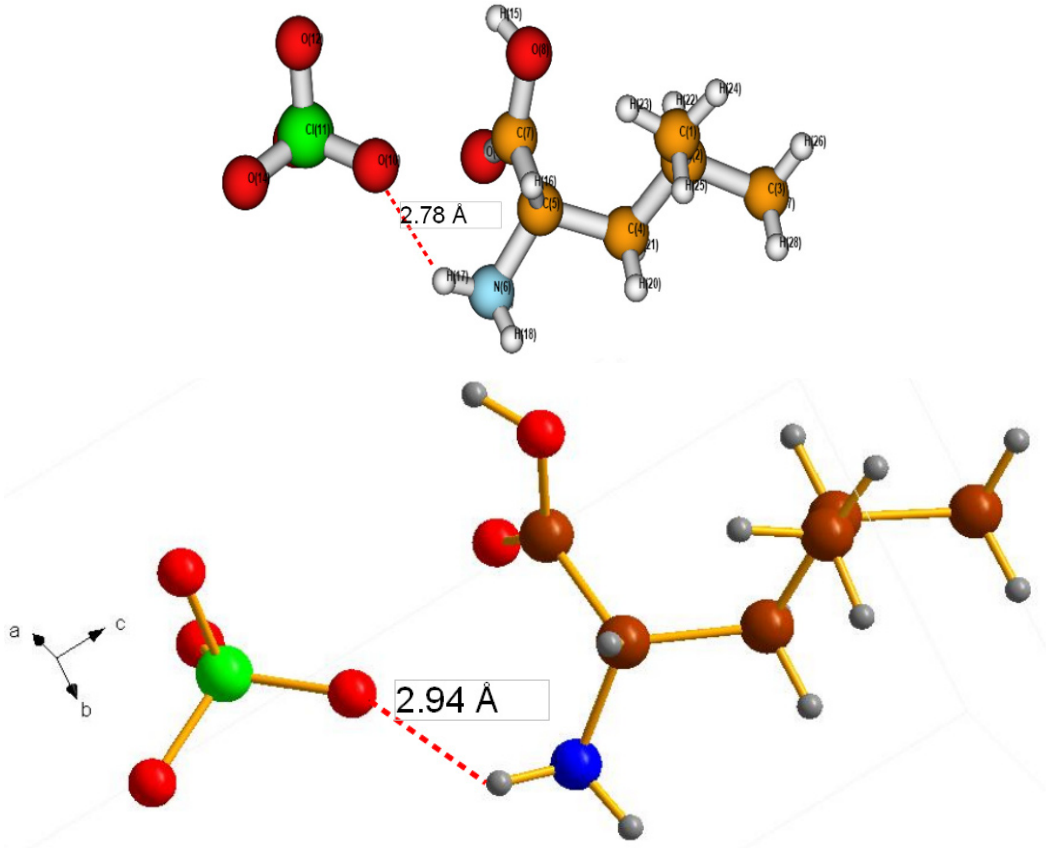

Figure 3. The equilibrium geometry of investigated molecule.

and the differences in particular Cl-O bond lengths are noticed. The experimental data are in the range 1.39 – 1.41 Å. The bigger differences are noticed among theoretical values. The shortest length (Cl11-O12) is equal to 1.47 Å, whereas the longest bond has 1.54 Å (Cl11-O13). The medium Cl-O bond lengths are equal to 1.49 and 1.52 Å for Cl11-O14 and Cl11-O10 bonds, respectively. The distortion from the tetrahedral geometry is confirmed by non-equivalent O-Cl-O angles obtained in theoretical calculation. These angles are in the range *ca.* 106 – 109°. Similar values were obtained from experimental study (106 - 115°).

According to theoretical approach one hydrogen bond of N-H…O type was noticed with length equals to 2.78 Å, whereas the corresponding experimental value is bigger and is equal to 2.94 Å. Obviously the DFT calculations cannot be adequate in the case of weak intermolecular interactions [25-27,33] however currently observed discrepancies are rather small.

The very good agreement is observed for experimental and theoretical values in the cases of intramolecular angles and dihedral agles (see Table 3). Bigger discrepancies are observed, only for angles described the N-H…O hydrogen bond.

3.5. Vibrational studies, theoretical PED analysis

Infrared and Raman spectra of powder samples of L-leucinium perchlorate acid complex are presented in Fig. 4. The observed (experimental) and theoretical wavenumbers, intensities, potential energy distribution and assignment are listed in Table 4. The theoretical IR and Raman spectra are shown in Fig. 5.

The crystal belongs to $P2_1$ space group with Z=2. From spectroscopic point of view the 165 bands should be active in both infrared and Raman spectra (82A' and 83 A"). We should remind that the molecule investigated in theoretical approach belongs to C_1 symmetry point group. The internal vibrations of the investigated compound may be analyzed taking into account the vibrations of the functional groups (CH_2, CH_3, CH, NH_3, COOH), hydrogen bonds (N…H-O) and of the perchlorate anion.

3.6. Vibrations of perchlorate anion

For isolated ClO_4^- group with T_d symmetry four bands (n_1, n_2, n_3 and n_4) in vibrational spectra should be observed. According to spectroscopic data the bands are noticed at: $n_3(F_2)$=1119 cm^{-1}, $n_1(A1)$ =928 cm^{-1}, $n_4(F2)$=625 cm^{-1} and $n_2(E)$=459 cm^{-1}. The n_3 and n_1 bands correspond

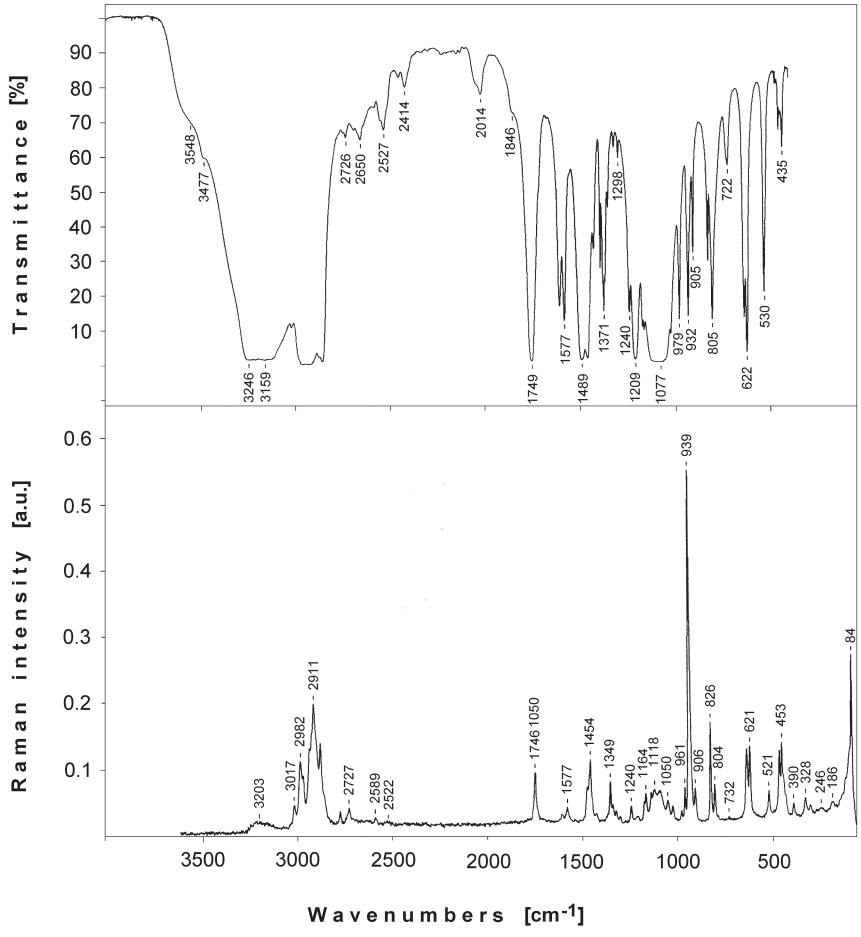

Figure 4. Room temperature powder FTIR (top) and FTRaman (bottom) spectra of L-leucinium perchlorate crystal.

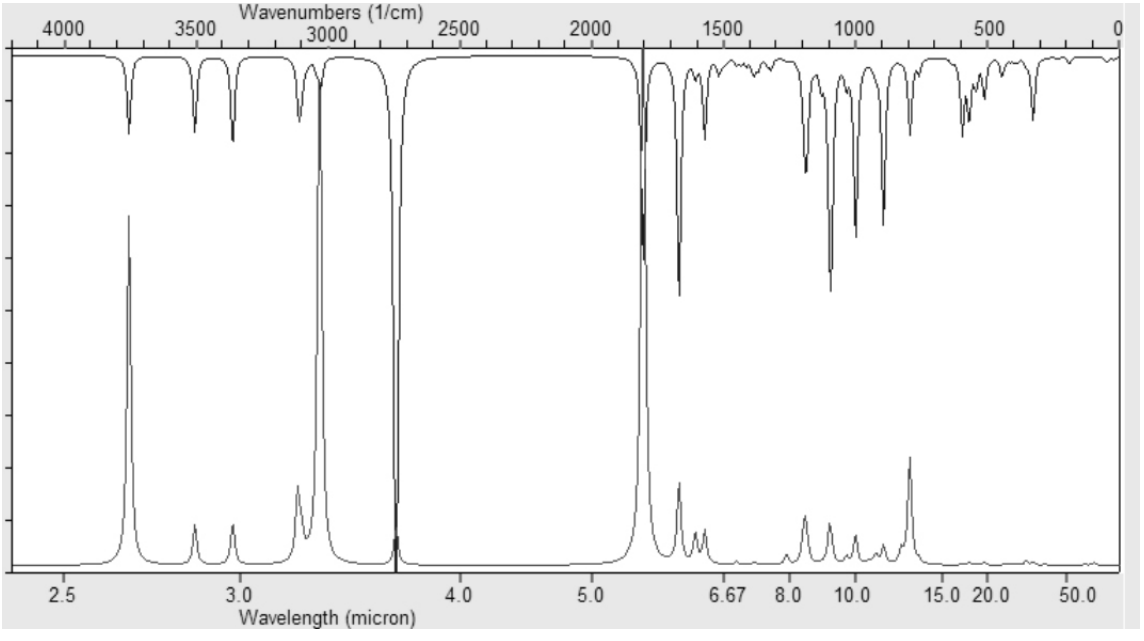

Figure 5. The thoretical vibrational spectra of investigated molecule.

Table 2. Natural Population Analysis.

Tab 4: Natural Population Analysis	
Atom No	**Natural charge**
C1	-0.70040
C2	-0.29139
C3	-0.68888
C4	-0.48023
C5	-0.17494
N6	-0.84360
C7	0.81032
O8	-0.69944
O9	-0.60733
O10	-0.87589
Cl11	2.44295
O12	-0.76448
O13	-0.87605
O14	-0.80641
H15	0.53095
H16	0.30954
H17	0.49819
H18	0.49739
H19	0.47028
H20	0.27826
H21	0.25076
H22	0.24533
H23	0.24267
H24	0.24772
H25	0.25386
H26	0.24893
H27	0.23939
H28	0.24251

to antisymmetric and symmetric stretching vibrations, respectively, whereas n_4 and n_2 bands are considered as originated from in-plane and out-of-plane deformation vibrations. In our studies the perchlorate anion cannot be described by the T_d symmetry point group, because all Cl-O distances are different and distortion from the tetrahedral is confirmed by the non-equivalent O-Cl-O angles. Due to lowering of symmetry from an ideal configuration the splitting of investigated bands as an effect of breaking of symmetry rules can be observed.

According to literature data, experimental spectra and PED analysis, the bands noticed at 1066 and 1059 cm^{-1} in theoretical spectrum were assigned to antisymmetric stretching vibrations of Cl-O bonds. The band corresponding to n_1 vibration was found at 971 cm^{-1}. The counterparts of these bands are observed in both experimental IR and Raman spectra. In this case very good agreement between experimental and theoretical data should be emphasized.

On the basis of PED analysis the bands originating from n_4 type of vibration are found at 868, 772 and 769 cm^{-1}. In experimental data the only one corresponding band was noticed (826 cm^{-1} in infrared and Raman spectra, respectively).

The bands noticed in theoretical spectrum at 553, 532, 526, and 402 cm^{-1} originate from n_2 type of vibration of perchlorate anion. In experimental spectra these bands are observed at 530 cm^{-1} (IR) and 521 cm^{-1} (Raman).

3.7. C-C vibrations of L –leucinium cation

The PED studies of the theoretical spectrum show that the bands originating from stretching C-C vibrations are noticed at 1005, 942, 803 and 769 cm^{-1}. Three of these bands have counterparts in Raman spectrum (1025, 979, 964 cm^{-1}). Three, different bands in infrared spectrum are observed, only (961, 932 and 805 cm^{-1}). From PED calculations it follows that these bands are complex in nature, mixed with band derived from C-N stretching vibration.

The theoretical band at 433 cm^{-1} was assigned to in-plane deformations of C-C-C skeletal. The experimental counterpart for this band is observed at 454 cm^{-1} in both Raman and IR spectra. The other bands originating from this type of vibrations are noticed at 422, 402, 375, 342, 228 and 129 cm^{-1}. For vibrations mentioned above the classification of symmetry is rather difficult.

3.8. C-H vibrations of L-leucinium cation

On the basis of PED calculations the classification of bands originating from different group (CH, CH_2 and CH_3) is simple. According to theoretical approach the bands noticed at 3020 and 3018 cm^{-1} correspond to antisymmetric stretching of C-H bonds of methyl group while the bands at 3012, 3004, 2944 and 2938 cm^{-1} to symmetric stretching one. The bands derived from symmetric C-H vibrations are noticed in Raman spectrum at 2934 and 2910 cm^{-1}. According to these studies, all C-H stretching vibrations are not mixed with any types of vibrations.

The PED analysis showed that band noticed at 2986 cm^{-1} with its counterpart in 2986 cm^{-1} (Raman, only) should be assigned to antisymmetric stretching vibrations of C-H bond of ethyl group. The band observed at 2935 cm^{-1} (2854 (IR), 2877 (Raman)) derives from symmetric stretching vibrations of above mentioned bond.

Table 3. Calculated geometric parameters for L-leucinium perchlorate. The data are compared with experimental values from [16].

Bond	Calculated Length [Å]	Experimental lengths [Å]	Angle	Calculated [°]	Experimental [°]	Dihedral angle	Calculated [°]	Experimental [°]
C1-C2	1.54	1.54	C1-C2-C3	110.89	109.58	C1-C3-C2-C4	-124.03	-122.72
C1-H23	1.09	0.96	C2-C1-H23	112.53	109.52	C2-C4-C5-C7	67.03	70.02
C1-H24	1.09	0.96	C2-C1-H24	110.20	109.47	C2-C4-C5-N6	-174.94	-170.62
C1-H25	1.10	0.96	C2-C1-H25	111.08	109.47	C3-C2-C4-C5	-177.08	-177.48
C2-C3	1.54	1.54	C2-C3-H26	110.61	109.48	C4-C2-C1-H23	-64.75	-64.08
C2-C4	1.54	1.55	C2-C3-H27	111.70	109.44	C4-C2-C1-H24	175.69	175.94
C2-H22	1.10	0.98	C2-C3-H28	111.01	109.49	C4-C2-C1-H25	56.11	56.03
C3-H26	1.09	0.96	C2-C4-C5	116.34	116.34	C4-C2-C3-H26	177.64	178.04
C3-H27	1.10	0.96	C3-C2-C4	108.81	109.92	C4-C2-C3-H27	57.57	58.02
C3-H28	1.10	0.96	C4-C2-H22	108.65	108.63	C4-C2-C3-H28	-62.93	-66.02
C4-C5	1.55	1.54	C4-C5-C7	113.03	111.86	C4-C5-C7-O8	-84.79	-84.68
C4-H20	1.10	0.97	C4-C5-N6	108.99	109.79	C5-C4-C2-H22	-60.11	-58.76
C4-H21	1.10	0.97	C5-C4-H20	106.30	108.22	C5-N6-O10-CL11	-77.28	123.18
C5-C7	1.52	1.53	C5-C4-H21	108.34	108.23	C7-C5-C4-H20	-171.99	-168.01
C5-H16	1.09	0.98	C5-C7-O8	112.69	113.26	C7-C5-C4-H21	-56.78	-51.94
C5-N6	1.50	1.53	C5-C7-O9	123.10	122.79	C7-C5-N6-H17	-76.90	-72.21
C7-O8	1.34	1.32	C5-N6-H17	111.01	109.43	C7-C5-N6-H18	171.64	167.72
C7-O9	1.22	1.22	C5-N6-H18	110.29	109.48	C7-C5-N6-H19	45.31	47.75
CL11-O12	1.47	1.39	C5-N6-H19	110.57	109.39	C7-C5-N6-O10	-116.88	-68.65
CL11-O13	1.54	1.41	C5-N6-O10	106.93	79.90	N6-C5-C7-O9	-25.32	-26.00
CL11-O14	1.49	1.41	C7-C5-H16	110.92	109.15	N6-O10-CL11-O12	-153.40	-142.74
N6-H17	1.03	0.89	C7-O8-H15	108.27	109.48	N6-O10-CL11-O13	-34.17	-21.91
N6-H18	1.07	0.89	N6-O10-CL11	90.63	131.90	N6-O10-CL11-O14	81.88	101.94
N6-H19	1.02	0.89	O10-CL11-O12	111.32	106.67	O9-C7-C5-H16	-141.08	-144.43
N6-O13	2.78	2.94	O10-CL11-O13	106.32	115.71	O9-C7-O8-H15	-0.88	28.04
O8-H15	0.97	0.82	O10-CL11-O14	109.03	109.15			
O10-CL11	1.52	1.39						

On the basis of PED analysis the band noticed at 3024 cm^{-1} with counterparts at 3215 and 3214 cm^{-1} in infrared and Raman spectra, respectively, was described as deriving from antisymmetric stretching vibration of C(5)-H(16) group, whereas band noticed at 2954 cm^{-1} (2953 cm^{-1} Raman) was assigned to stretching vibration of C(2)-H(22) band.

The bands recognized as deriving from in-plane deformations of CH groups are noticed in the wide range of vavenumbers (1475 – 1410 cm^{-1}). The counterparts of these bands are noticed in both experimental infrared and Raman spectra. These values of obtained frequencies are typical and are in very good agreement with experimental data. For this type of vibrations the percentage in potential energy distribution is very high.

According to PED analysis the frequencies noticed in the range 1393 – 1122 cm^{-1} are assigned to rocking type of vibrations of C-H bonds. The PED study showed that almost all these vibration can be regarded as "pure".

The bands noticed at 942, 922, 908 and 895 cm^{-1} are assigned to out-of-plane deformations type of C-H bonds. In these bands the pronounced participation of other types of vibrations is also observed.

On the basis of PED calculation the low frequency bands at 266 and 220 cm^{-1} derive from twisting (t) type of vibrations of C-H bonds. In experimental spectrum one band at 245 cm^{-1} was observed in this range.

3.9. C-N vibrations of L-leucinium cation

According to theoretical calculation the frequency derived from stretching vibrations of C-N bonds are noticed at 1005 cm^{-1} (antisymmetric) and 968 cm^{-1} (symmetric). As bands originating from this type of vibrations in infrared spectra the ones at 1020 and 961 cm^{-1} were proposed.

Table 4. Calculated frequencies and PED analysis.

Calculated Scaled frequency	Calculated intensity		Experimental		PED [%]	assignment
	IR [km mol^{-1}]	Raman [Å^4 AMU^{-1}]	IR	Raman		
3644	105	422054			O8-H15 100	nOH
3401	113	49209	3595wsh		N6-H19 93	$n_{as}NH_3$
3262	134	52561	3474w		N6-H17 93	n_sNH_3
3024	10	74010	3017vs	3214vwb	C5-H16 76, C1-H23 17	n_aCH
3020	42	4455		3017vw	C3-H26 42, C3-H27 30, C1-H23 13, C1-H24 11	n_aCH_3
3018	17	1110			C1-H23 45, C3-H26 16, C5-H16 16	$n_{as}CH_3$
3012	38	26865			C1-H24 42, C1-H25 34, C3-H27 11	n_sCH_3
3004	21	13181			C3-H28 37, C3-H27 23, C3-H26 19	n_sCH_3
2986	9	4778		2982m	C4-H20 50, C4-H21 39	n_aCH_2
2954	17	83		2953w	C2-H22 81	n_sCH
2944	7	454764		2934m	C1-H25 46, C1-H24 22, C1-H23 17	n_sCH_3
2938	34	232022		2910s	C3-H28 35, C3-H27 14, C4-H20 13, C4-H21 13, C3-H26 13	n_sCH_3
2935	9	5897		2877vw	C4-H21 37, C4-H20 32, C3-H28 16	n_sCH_2
2661	1087	47533		2772vw	N6-H18 96	nNH...O
				2727vw		
1753	296	890812	1749vs	1746w	C7-O9 85	$n_aC{=}O$
1621	375	99737	1602vs	1608vw	C7-C5-N6-H18 47, C7-C5-N6-H17 33	dNH_3
1560	25	37367	1577vs	1579vw	C7-C5-N6-H19 35, C5-N6-H17 34, C7-C5-N6-H17 10	dNH_3
1526	116	39583	1512s		C5-N6-H18 60, C5-N6-H19 17, C5-N6-H17 12	dNH_3
1475	21	69	1482vs	1472vw	C4-C2-C1-H23 30, C4-C2-C1-H24 23, C4-C2-C3-H27 11	dCH_3
1466	6	12	1462vs		C4-C2-C3-H28 31, C4-C2-C1-H25 15, C4-C2-C3-H26 14	dCH_3
1456	4	39	1455vs	1455w	C4-C2-C3-H26 27, C4-C2-C1-H24 16, C4-C2-C1-H25 13, C4-C2-C3-H27 11	dCH_3
1451	2	78			C7-C5-C4-H20 16, C4-C2-C3-H27 15, C7-C5-C4-H21 14, C4-C2-C1-H23 14	dCH_2, dCH_3
1443	3	2	1424m	1425vw	C7-C5-C4-H20 15, C4-C2-C1-H25 14, C4-C2-C3-H28 13, C7-C5-C4-H21 12, C4-C2-C3-H27 10	dCH_2, dCH_3
1410	9	3454			C7-C5-H16 19, O9-C7-C5-H16 14, C5-C7 11, C7-O8 11	dCH, n_sCO
1393	8	26	1390s		C2-C1-H25 20, C2-C3-H27 15, C2-C3-H28 15, C2-C1-H24 15, C2-C1-H23 14, C2-C3-H26 14	rCH_3
1373	9	8	1372s		C2-C3-H28 19, C2-C1-H25 17, C2-C3-H26 17, C2-C3-H27 16, C2-C1-H23 13, C2-C1-H24 12	rCH_3
1352	10	413	1350w	1350w	C4-C2-H22 44, C5-C4-H20 19	rCH_2 defCH
1343	19	2353		1338vw	O9-C7-C5-H16 38, C5-C4-H21 25	rCH_2
1328	16	1019	1319w	1318vw	C5-C4-C2-H22 21, O9-C7-C5-H16 16, C5-C4-H21 10, C4-C2-H22 10	rCH_2 defCH
1296	9	277	1298w	1298vw	C5-C4-C2-H22 41, C5-C4-H21 16, C7-C5-H16 11	rCH_2 defCH
1281	16	1144	1240s	1240vw	C5-C4-H20 22, C4-C2-H22 17, C7-O8-H15 16	rCH_2 defCH
1224	4	12523	1209vs	1204vw	C7-C5-H16 22, C5-C4-H20 10	rCH_2 defCH
1163	31	23927	1173vs	1173vw	C1-C2 9,C5-N6-H19 8, C5-N6-H17 7, C2-C3-H27 7, C2-C4-C5-C7 7, C2-C1-H25 7	n_a defCH

Continued **Table 4.** Calculated frequencies and PED analysis.

Calculated Scaled frequency	Calculated intensity IR [km mol^{-1}]	Calculated intensity Raman [Å^4 AMU^{-1}]	Experimental IR	Experimental Raman	PED [%]	assignment
1156	97	39079	1163vs	1165vw	C7-O8-H15 17, C7-O8 13, C2-C1-H23 8, C1-C2-C3 7, C2-C1-H24 6	n_sCO, defCH
1149	86	12166		1136vw	C7-O8-H15 16, C7-O8 16, C5-N6-H17 9	n_a CO, defCH, rNH_3
1122	6	16		1118vw	C7-C5-H16 16, C4-C2-H2 29, C2-C4 9, C2-C3-H2 8, C5-C4-H2 7	rCH_2
1098	33	1780	1092vsb	1091vw	C5-N6-H19 14, C5-N6-H18 14, C7-C5-H16 12	wNH_3
1066	184	44441			CL11-O12 43, CL11-O14 7	$n_a$$ClO_4$
1059	204	11863		1050vw	CL11-O12 29, C5-N6-H19 14, CL11-O14 7	$n_a$$ClO_4$, w$NH_3$
1005	34	8908	1024vs	1025vw	C5-N6 50, C4-C5 14	n_aCN, nCC
971	242	35505	978vs	978vw	CL11-O14 52, O10-CL11 17, CL11-O12 5	$n_s$$ClO_4$
968	23	129	961wsh	961vw	C4-C5 20, C5-N6 14, C2-C4 13, C5-C7 7	nCN
942	1	909	932s	932vs	C2-C1-H24 23, C2-C3 21, C2-C3-H26 16, C1-C2 11	wCH_3, nCC
922	1	3179			C2-C3-H27 19, C2-C4 18, C2-C3 13, C4-C5 7	nCC, wCH_3
908	4	2743	906m	906vw	C2-C1-H23 20, C2-C3-H28 19, C2-C1-H25 15, C5-C4-C2-H22 12	wCH_3
895	15	10923			C2-C4-C5-C7 13, C7-C5-C4-H20 10, C7-C5-C4-H21 9	wCH_3, wCH_2
868	244	23094	826m	825w	O10-CL11 45, CL11-O13 23, CL11-O14 7	$n_4$$ClO_4$
803	3	16134	805vs	vw	C1-C2 36, C2-C3 17, C2-C4 16	nCC
772	54	119149			CL11-O13 37, C5-C7 12, O10-CL11 10, CL11-O12 7, CL11-O14 7	$n_4$$ClO_4$
769	60	11887			CL11-O13 23, C5-C7 21, O10-CL11 6	$n_4$$ClO_4$, nCC
737	21	5316			N6-C5-C7-O9 27, C4-C5-C7-O8 19, O9-C7-O8-H15 18	defCOO
617	6	208	637s	638w	C5-C7-O9 55, C7-O8 11, C2-C4-C5-N6 9, C2-C4-C5-C7 7	defCOO
578	107	956	622vs	621w	O9-C7-O8-H15 79	defCOH
553	82	3323			O10-CL11-O13 41, N6-O10-CL11-O13 23, O10-CL11-O14 20, N6-O10-CL11-O14 16	$n_2$$ClO_4$
532	12	1204	530s		N6-O10-CL11-O14 26, O10-CL11-O12 22, O10-CL11-O14 21, N6-O10-CL11-O12 19	$n_2$$ClO_4$
526	27	440		521vw	N6-O10-CL11-O13 33, O10-CL11-O12 29 O10-CL11-O13 19 N6-O10-CL11-O12 14	$n_2$$ClO_4$
497	57	3195		467w	C5-C7-O8 30, C4-C5-N6 11, C5-N6 10	defCCO, defCCN
433	28	116	454vw	454w	C1-C3-C2-C4 16, C4-C5-N6 14, O10-CL11-O14 13	Skeletal CCC, defCCN
422	5	1384	434w	447w	C1-C2-C3 36, C2-C4-C5 11, C3-C2-C4 8	defCCC
402	4	1185			C1-C3-C2-C4 27, O10-CL11-O13 20, O10-CL11-O14 19, N6-O10-CL11-O12 12, C5-C7-O8 10	Skeletal CCC, $n_2$$ClO_4$
388	4	620		391vw	O10-CL11-O12 29, O10-CL11-O13 15, N6-O10 11, N6-O10-CL11-O13 11, N6-O10-CL11-O14 9	defClO_4 bridgeN6-O10(2.78Å)

Continued **Table 4.** Calculated frequencies and PED analysis.

Calculated Scaled frequency	Calculated intensity IR [km mol^{-1}]	Calculated intensity Raman [Å^4 AMU^{-1}]	Experimental IR	Experimental Raman	PED [%]	assignment
375	4	433			O10-CL11-O14 16, C3-C2-C4 13, C4-C5-N6 12, C1-C3-C2-C4 11, O10-CL11-O12 11	Skeletal CCC, CCN_{def}, $defClO_4$
342	9	5625		329vw	C1-C2-C3 24, C3-C2-C4 15, N6-O10 10	Skeletal CCC
318	94	2800		304vw	N6-O10 19, C2-C4-C5-N6 19, C5-C7-O9 15, C5-C7-O8 11, N6-O10-CL11 11	Skeletal,defCOO
273	0	1466			C5-C7-O8 14, C4-C5-N6 13, C2-C4-C5 11	defCCO, defCCN
266	2	4		245vw	C4-C2-C1-H25 18, C4-C2-C1-H23 17, C4-C2-C1-H24 16, C4-C5-C7 15	tCH_3
228	4	220			C4-C5-C7 20, C2-C4-C5-C7 9, C4-C2-C1-H25 9	Skeletal CCC
220	0	57			C4-C2-C3-H26 28, C4-C2-C3-H28 27, C4-C2-C3-H27 26	tCH_3
184	11	5		189vw	N6-O10-CL11 28, C4-C5-N6 16, C2-C4-C5 12, N6-O10 10, C3-C2-C4 9	bridgeN6-O10(2.78Å), tNH_3
129	2	1210		119vw	C2-C4-C5 30, C4-C5-C7 27, N6-O10-CL11 14, C2-C4-C5-N6 14	Skeletal
108	2	263			C3-C2-C4-C5 28, C4-C5-C7-O8 20, C2-C4-C5-N6 15, N6-O10 11, C5-N6-O10 10	Skeletal
92	2	2990			N6-O10 42, N6-O10-CL11 13	bridge N6-O10 (2.78Å), tNH_3
53	4	50			C5-N6-O10-CL11 38, C2-C4-C5-C7 16, N6-O10-CL11-O13 14, C3-C2-C4-C5 12	Skeletal
46	4	105			N6-C5-C7-O9 29, C3-C2-C4-C5 27, C4-C5-C7-O8 21	$COO_{def.}$
39	2	4			C5-N6-O10 52, C2-C4-C5-C7 15, C5-N6-O10-CL11 12	bridgeN6-O10(2.78Å)$_{def.}$
29	0	2			C5-N6-O10-CL11 27, N6-O10-CL11-O14 23 N6-O10-CL11 21, N6-O10-CL11-O12 15, C7-C5-N6-O10 12	skeletal
22	3	5			C7-C5-N6-O10 41, C5-N6-O10 34, C2-C4-C5-N6 22	skeletal
6	3	1			C7-C5-N6-O10 35, C2-C4-C5-N6 28, C5-N6-O10 17, C2-C4-C5-C7 11	skeletal

Abbreviations: n - stretching, s – s\ymmetric, a – antisymmetric, s - scissoring symmetric in-plane), r - rocking antisymmetric in –plane), w - wagging (symmetric out-of plane), t - twisting (antisymmetric out-of-plane), def - deformation.

The Raman counterparts of these bands are noticed at 1025 and 979 cm^{-1}, respectively.

The bands arising from deformation vibrations of CCN groups are noticed at 497, 433, 375 and 273 cm^{-1}. These frequencies are comparable with values obtained in previous calculation. The detailed PED analysis suggests strongly that in low frequency bands observed below 108 cm^{-1} the medium participation of the deformation vibration of CCN skeleton takes place.

3.10. C-O vibrations of L-leucinium cation

The bands originating from stretching vibrations of carbonyl group were assigned on the basis of PED analysis. The band arising from $n_{as}C=O$ vibration should be observe in the range of 1750 – 1650 cm^{-1}. On the basis of PED analysis the frequency noticed at 1753 cm^{-1} was assigned to antisymmetric stretching vibration of C=O bond. The PED calculation showed that this band is not mixed (the 85% potential energy contribution of C7-O9 bond vibration). The analysis of experimental spectra corroborates this result. The band at 1749 cm^{-1} observed in infrared spectrum arising from $n_{as}C=O$ vibration, whereas this band in Raman spectrum is noticed at 1746 cm^{-1}. In the theoretical calculation it was assumed that proton is connected with CO group. The good agreement between experimental spectra

and results of theoretical calculations shows that in real crystal the carbonyl group is protonated.

The bands arising from n_sC=O vibrations of COOH group are noticed at 1410, 1156, and 1149 cm^{-1}. The PED analysis confirms that these bands are not "pure". The experimental counterparts of these bands are observed at 1163 cm^{-1}(IR) and 1165, 1136 cm^{-1} (Raman).

The frequencies for deformation vibrations of COOH group are obtained on the basis of PED analysis at 737, 617, 578 and 497 cm^{-1}. It should be noticed that three from above bands are not mixed. In measured infrared spectrum these bands are located at 637, 622 and 474 cm^{-1}. The Raman counterparts of these bands are present at 638, 621 and 467 cm^{-1}. According to PED calculation, the typical frequencies for out-of-plane deformations of COOH group are obtained at 318 and 273 cm^{-1}, but clear-cut interpretation of these results seems to be very difficult because the bands are strongly mixed. In measured spectra only one band was assigned to this type of vibrations (at 304 cm^{-1} in Raman spectrum).

3.11. N-H vibrations of L-leucinium cation

In the real crystal five N-H..O hydrogen bonds are formed. The lengths of these bonds are in the wide range of 2.852 – 3.041 Å [16]. Three protons connected with N6 are involved in this interaction. For two protons the bifurcated hydrogen bonds are created. In theoretical approach only one N(6)-O(13) hydrogen bond is noticed. The length of this bond in theoretical calculation was 2.94 Å. On the basis of PED analysis the band originating from stretching vibration of this N-H…O bond is noticed at 2661 cm^{-1}. Because in real crystal the hydrogen bond with similar length is observed, therefore the band at 2727 cm^{-1} present in infrared spectrum was assigned to this type of vibration. The participation of N-H…O deformation vibrations is observed in bands arising from skeletal vibrations of investigated molecule. The low frequency bands noticed at 184, 92 and 39 cm^{-1} originate from this type of vibrations, but its assignment in real spectra is questionable.

On the basis of theoretical calculation the frequencies noticed at 3401 and 3262 cm^{-1} were assigned to n_{as}NH and n_sNH vibration, respectively. Surprisingly, the counterparts of these bands were not found in infrared spectrum. The corresponding bands are noticed at 3595 and 3474 cm^{-1}.

The PED analysis shows that the bands arising from deformation in-plane type of vibrations of the amino group should be observed at 1621, 1560 and 1526 cm^{-1}. The bands are not mixed. The percentage contribution in PED for this type of vibrations is bigger than 90%. For all these bands the appropriate one in real spectra were found. In such a case the theoretical and experimental results are in excellent agreement.

The region of rocking vibrations of NH_3 group exhibits in experimental Raman spectrum a lot of bands. On the basis of PED approach the frequencies at 1163 and 1149 cm^{-1} were assigned to rNH_3 type of vibrations. All bands are mixed. In experimental spectra the bands are noticed at 1173 cm^{-1} (IR and Raman) and 1136 cm^{-1} (Raman only).

According to PED results the bands observed at 1089 and 1059 cm^{-1} were assigned partially to wNH_3 type of vibrations. The bands observed at 1092 and 1024 cm^{-1} in infrared spectrum arise from this type of vibrations and have Raman counterparts at 1096 and 1050 cm^{-1}, respectively.

The clear-cut assignment of tNH_3 type of vibrations in real spectra on the basis of PED calculation is rather difficult. Bands are observed at 375, 184 and 92 cm^{-1} due to this type of vibrations. The counterparts of these bands are observed in Raman spectrum.

4. Conclusions

1. L-leucinium perchlorate crystals can be used as second harmonic generator. These properties were confirmed by Kurtz-Perry experiment as well as by theoretical calculations.

2. Good agreement between experimental (x-ray) and theoretical (DFT) structure is observed. The small discrepancies are observed in geometry of hydrogen bonds, only.

3. Clear-cut assignment s of observed in vibrational spectra bands were made on the basis of the potential energy distribution (PED) analysis. Generally, the experimental spectra confirm the geometry of complex obrained by X-ray method.

4. On the basis of DSC measurement the thermal instabilities close to 200 K were observed.

Acknowledgement

The calculations were performed with the aid of the computers in the Wrocław Supercomputer and Networking Center. The work was financially supported by National Science Centre (Project No. N N507 221840).

References

[1] L.G. Koreneva, V.F. Zolin, B.L. Davydov, Nonlinear Optics of Molecular Crystals (Moscow, Nauka, 1985) (in Russian)

[2] J.F. Nicoud, R.J. Tweig, In: D.S. Chemla, J. Zyss (Eds.), Nonlinear Optical Properties of Organic Molecules and Crystals, Vol. 1 (Academic Press, London, 1987)

[3] D. Xu, M. Jiang, Shandong Daxue Xuebao, Ziran Kexueban, 23, 103 (1988); Chem. Abstr. 110, 67141 (1989)

[4] D. Eimerl, S. Velsko, L. David, F. Wang, G. Loiacono, G. KennedyIEEE, J. Quantum Electron 25, 179 (1989)

[5] A. Yokotani, T. Sasaki, K. Fujioka, S. Nakai, C. Yamanaka,J. Cryst. Growth 99, 815 (1990)

[6] S. Dhanuskodi, P.A. Angeli Mary, K. Vasantha, Spectrochim. Acta A59, 927 (2003)

[7] G. Dhanaraj, T. Shripathi, H. L. Bhat, J. Crystal. Growth 113, 456 (1991)

[8] S.B. Monaco, L.E. Davis, S.P. Velsko, F.T. Wang, D. Eirmel, A. Zalkin, J. Cryst. Growth 85, 252 (1987)

[9] A.M. Petrosyan, R.P. Sukiasyan, S.S. Terzyan, V.M. Burbelo, Acta Cryst. B55, 221 (1999)

[10] S. Haussühl, Z. Kristallogr. 188, 311 (1989)

[11] G. Ashaak, Ferroelectrics 104, 147 (1990)

[12] I. Nemec, Z. Micka, J. Mol. Struct. 563-564, 295 (2001)

[13] K. Rajagopal, R.V. Krishnakumar, M.S. Nandhini, R. Malathi, S.S. Rajan, S. Natarajan, Acta. Cryst E 59, o878 (2003)

[14] M. Anbuchezhiyan, S. Ponnusamy, C. Muthamizhchelvan, Optoelectronics and Advanced Materials – Rapid Communications 3(11), 1161 (2009)

[15] K. Anitha, S. Athimoolam, R. K. Rajaram, Acta Cryst. E61, o1604 (2005)

[16] J. Janczak, G. J. Perpetuo, Acta Cryst. C 63, part 2, o117 (2007)

[17] G. Fogarasi, P. Pulay, In: J.R. During (Ed.), Vibrational Spectra and Structure (Elsevier, New York, 1985) Vol. 13

[18] W. Zierkiewicz, D. Michalska, Th. Zeegers-Huyskens, J. Phys. Chem. A104, 11685 (2000)

[19] S. Kucharski, J.R. Bull. Polish. Acad. Sci. (Chem.) 45, 319 (1997)

[20] M.W. Schmidt, K.K. Baldridge, J.A. Boatz, S.T. Elbert, M.S. Gordon, J.H. Jensen, S. Koseki, N. Matsunaga, K.A. Nguyen, S.J. Su, T.L. Windus, M. Dupuis J.A. Montgomery, J. Comput. Chem. 14, 1347 (1993)

[21] H. Siebert, Z. Anorg. Allg. Chem. 275, 225 (1954)

[22] M. Drozd, M.K. Marchewka, Spectrochim. Acta A 64, 6 (2006)

[23] S.K. Kurtz, T.T. Perry, J. Appl. Phys. 39, 3798 (1968)

[24] H.M. Badawi, J. Mol. Struct. 984, 209 (2010)

[25] R.M. Dreizler, E.K.U. Gross, Density Functional Theory An Approach to the Quantum Many-Body Problem (Springer-Verlag, Berlin, Heidelberg, 1990)

[26] R.G. Parr, W. Yang, Density-Functional Theory of Atoms and Molecules (Oxford University Press, New York/ Clarendon Press, Oxford, 1989)

[27] W. Koch, M.C. Holthausen, A Chemist's Guide to Density Functional Theory, 2nd Edition (Wiley-VCH, Weinheim, 2001)

[28] D.C. Young, Computational Chemistry: A Practical Guide for Applying Techniques to Real-World Problems (John Wiley and Sons, New York, 2001)

[29] J.P. Lowe, K.A. Peterson, Quantum Chemistry (Elsevier, Amsterdam, 2006)

[30] D.W. Rogers, Computational Chemistry Using the PC (Wiley-Interscience, New York, 2003)

[31] K.I. Ramachandran, G. Deepa, K. Namboori, Computational Chemistry and Molecular Modeling Principles and Applications (Springer-Verlag, Berlin, Heidelberg, 2008)

[32] L. Piela, Ideas of Quantum Chemistry (Elsevier, Amsterdam, 2007)

[33] M. Mueller, Fundamentals of Quantum Chemistry, Molecular Spectroscopy and Modern Electronic Structure Computations (Kluwer Academic Publishers, New York, Boston, Dordrecht, London, Moscow, 2001)

[34] C.J. Cramer, Essentials of Computational Chemistry, Theories and Models, 2nd edition (John Wiley and Sons, Chichester, 2004)

[35] J.B. Foresman, AE Frisch, Exploring Chemistry With Electronic Structure Methods: A Guide to Using Gaussian (Gaussian, Inc., Pittsburgh PA, 1996)

[36] M.K. Marchewka, M. Drozd, A. Pietraszko, Mat. Sci. Eng. B100, 225 (2003)

[37] M. Drozd, M.K. Marchewka, Cent. Eur. J. Chem. 8(6), 1192 (2010)